Proceedings of the 7th European VLBI Network Symposium
Bachiller, R. Colomer, F., Desmurs, J.F., de Vicente, P. (eds.)
October 12th-15th 2004, Toledo, Spain

A follow-up RM observation for helical magnetic field in 3C 273

K. Asada[1,2] and M. Inoue[1]

[1] National Astronomical Observatory of Japan, 2-21-1, Osawa, Mitaka, Tokyo, 181-8588, Japan
[2] Graduate University for Advanced Studies, 2-21-1, Osawa, Mitaka, Tokyo, 181-8588, Japan

Abstract. We present results of our follow-up observation for a gradient of Faraday Rotation Measure (RM) across 3C 273 jet. We have found RM gradient across 3C 273 jet, and it may reveals a presence of a helical magnetic field which has been suggested to be related to the formation and collimation of jets by magneto-hydrodynamic models. However, regime we could reveal a distribution of RM was very limited, since 3C 273 was observed as a calibrator. In order to reveal further distribution of RM, we made follow-up observation. We detected gradient of RM across the jet and it continues more than 20 pc in projected distance. In addition, the distribution of the RM shows a significant proper motion. Coincidentally, its apparent proper motion of 5.25 c corresponds to that of the relativistic emitting plasma of 5.26 c.

1. Introduction

The studies for acceleration and collimation mechanism of AGN jets have been one of the primary targets for VLBI observers. The studies was started with discovery of superluminal motions, and a continual progress have been made more than thirty years. However we still do not know what is important for acceleration and collimation of the jets. From a theoretical point of view, several models are proposed. For the acceleration of the jets, jets driven by radiative pressure force (e.g., Sikora et al. 1996) or magnetic field (e.g., Meier et al. 2001) have been mainly discussed. In the jet driven by magnetic force, the toroidal component of the magnetic field is crucial for the collimation process, and both the acceleration and collimation of the jets would be simultaneously explained. On the other hand, from a observational point of view, VLBA and VSOP observations have been providing some evidence in support for the MHD models (Junor et al. 1999; Gabuzda 2000; Gabuzda et al. 2000). It is, however, not simple to see the toroidal component or helical magnetic field by observing the distributions of brightness or projected direction of the magnetic field. One of the effort that VLBI observers can make is revealing 3D structure of the magnetic field in the AGN jets based on VLBI polarimetry. Since emission from the jet is due to the synchrotron radiation, polarization position angle (PA) is perpendicular to the magnetic field in the optically thin region. In addition, Faraday Rotation Measure (RM) is related to the electron density $n_{\rm e}$, and the line of sight component of the magnetic field, $B_{\parallel}$, as $RM \sim \int_{LOS} n_{\rm e} B_{\parallel} dr$, where $\int_{LOS} dr$ represents integration along the line of sight. With the combination of the distributions of PA and RM, we can estimate 3D structure of the magnetic field in the jet. For this purpose, we started this study using VLBA archival data, and found the gradient of the RM across the VLBI jet of well-known quasar, 3C 273 (Asada et al. 2002; Here after KA02). The gradient of RM would be attributed to the toroidal component of the magnetic field or the helical magnetic field (KA02). Following our discovery, the gradient of the RM across jets are reported for several VLBI jets (Gabuzda et al. 2004; Zavala & Taylor 2004). It is, however, the region where KA02 revealed the distribution of RM are only one knot in the long jet, since 3C 273 was observed as one of the calibration sources. Full track observation would be promising in order to confirm the transverse gradient of the RM and obtain the detailed distribution of RM. We present here the results of our follow-up VLBA polarimetry towards 3C 273.

The well-known quasar 3C 273, at a redshift of z = 0.158 (Schmidt 1963), is one of the brightest quasars. For the Hubble constant of H0 = 100 km s^{-1} Mpc^{-1} and deceleration parameter of $q_0 = 0.5$, an angular resolution of 1 mas corresponds to a linear resolution 1.86 pc. The jet components in 3C 273 were found as superluminal motions based on one baseline VLBI (Whiteny et al. 1971, Cohen et al. 1971), with the speeds of the apparent proper motion being 4.9 to 7.7 c derived from VLBI monitoring observation (Abraham et al. 1996).

2. Observation and Data Reduction

Observations were carried out on 15 December 2002 using all ten stations of the VLBA. In order to arrange observing wavelength to be a minimum redundancy in λ^2 space in each band, we chose IF frequencies of 4.618, 4.688, 4.800, and 5.093 GHz in the 5-GHz band, and at 8.118, 8.188, 8.402, and 8.593 GHz in the 8-GHz band. Each IF has an 8-MHz bandwidth. Both left and right circular polarizations were recorded at each station. The integration time towards 3C 273 was 66 minutes at each frequency. We observed OQ 208 as an instrumental calibration source, and 3C 279 and 4C 29.45 as polarization position angle calibration source.

An a priori amplitude calibration for each station was derived from a measurement of the antenna gain and system temperatures during each run. Fringe fitting was performed on each IF and polarization independently using AIPS task FRING. After deriving the delay and rate difference between parallel-hand cross correlations, the cross-hand correlations were fringe fitted to determine the cross-hand delay difference. Once the cross-hand delay difference was determined, full self-calibration was performed for parallel-hand cross correlations.

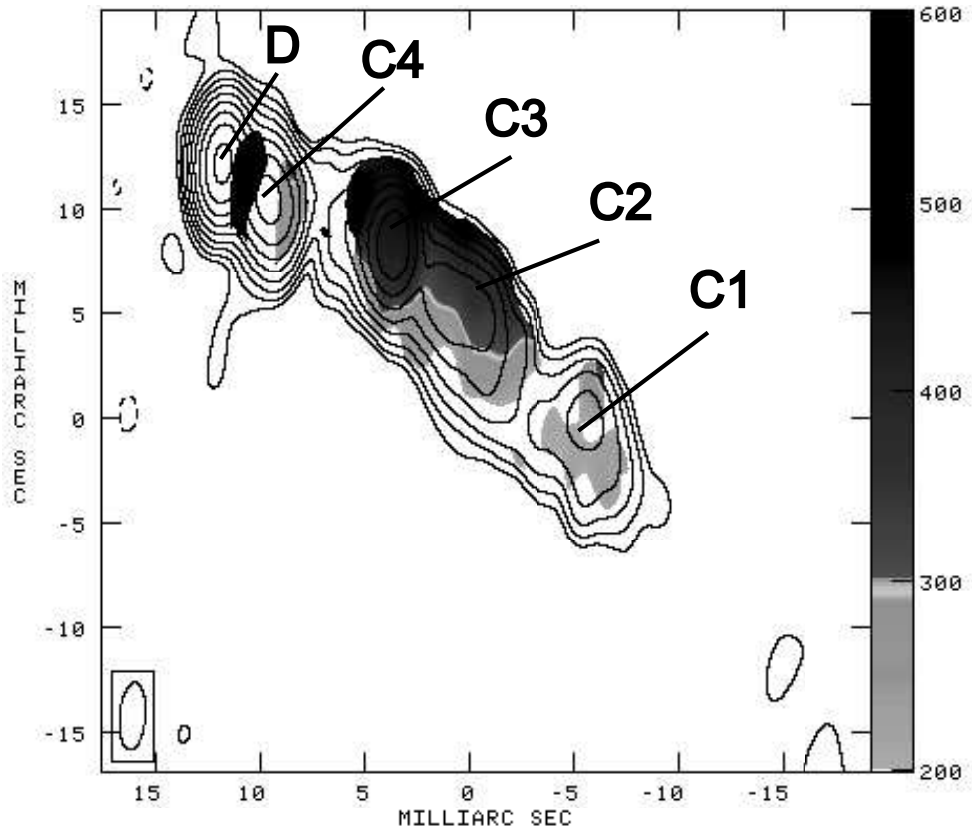

Fig. 1. Distribution of RM (grey scale) superposed on the contour images of the total intensity at 4.618 GHz. Contours are plotted at -1, 1, 2, 4, 8, 16, 32, 64, 128, 256, 512 and 1024 × three-times the r.m.s. noise of that of the total intensity at 4.618 GHz. The synthesized beam size is restored by the 4.618 GHz beam of 3.2 mas × 1.2 mas with the major axis at a position angle of - 4°.7. The RMs are plotted in the region where the polarized intensity is greater than 3-times the r.m.s. noise in the polarized intensity.

Images were initially obtained using DIFMAP, and then imported into AIPS to self-calibrate the full data sets using the task CALIB and the final DIFMAP image. The instrumental polarizations of the antennas were determined for each IF at each band with OQ 208, using AIPS task LPCAL. The polarization angle offset at each station was calibrated using 3C 279 obtained by VLA/VLBA Polarization Calibration Monitoring Program (Myers & Taylor). The source was observed on 17 Dec 2003 by VLA at 4.8851 and 4.8351 GHz and 8.4351 and 8.4851 GHz. The difference between the two observations is presumably small, since the observations were made with VLA and VLBA within 2 days. Since observing frequencies are slightly different between VLA and VLBA observations, VLBA polarization position angles were interpolated using the VLA polarization position angle. In order to obtain the distributions of RM and projected magnetic field, we restored images at higher frequencies to match the resolution at lowest frequency observation. The restored beam size was 3.22 mas × 1.23 mas with the major axis at a position angle of - 4.°63.

For the registration of images at different frequencies, we identified four distinct components. We measured the relative position with respect to the core component, peak flux, integrate flux, and size by AIPS task IMFIT. As the core position may be shifted with frequency by synchrotron self-absorption (Blandford & Konigl 1979), we used optically thin components to register images at different frequency. We derived the positions of these components by weighted signal-to-noise ratio. The variances of the position of optically thin components are 0.059 mas in RA and 0.061 mas in Dec. Those are 0.05 × and 0.02 × the beam size, respectively. The distribution of RM was obtained by AIPS task RM with polarization images at 4.618, 5.093, 8.118, and 8.593 GHz, with regions where the polarized intensity is greater than three times the r.m.s. noise in the polarized intensity.

Table 1. Apparent proper motion

Component	β_{app}	θ_{max}
C1	5.90 ± 0.03	19°.2 ± 0°.1
C2	5.26 ± 0.01	21°.5 ± 0°.1
C3	7.24 ± 0.01	15°.7 ± 0°.1

3. Results

3.1. Apparent motion of the jet

We show the distribution of RM in figure 1. We identified five components in the jet and labeled jet in the same manner as that at the first epoch (KA02). We measured its apparent velocities β_{app} with respect to the core component D and details are listed in table 1. The apparent velocities are consistent with the appar-

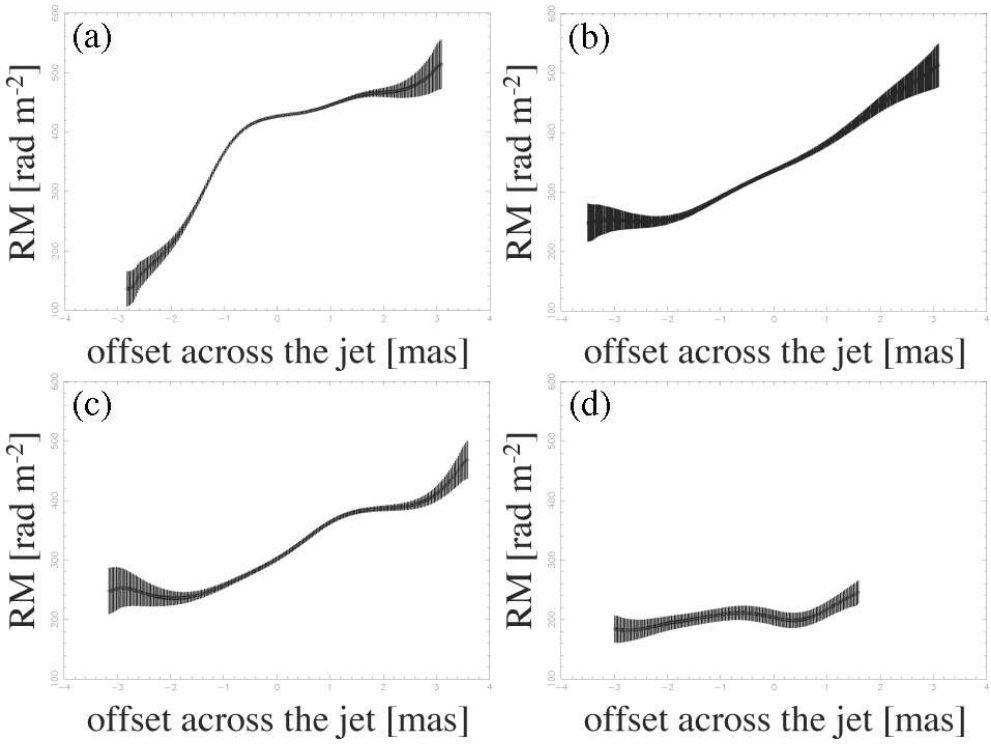

Fig. 2. Cross sections of the RM distribution across (a) C3 (b) C2 upper side (c) C2 lower side and (d) C1 in the second epoch derived using the AIPS task SLICE. The shaded area along the curved line of RM indicates the standard deviation (1 σ) in RM. The profile of the RM distribution is anti-symmetric with respect to the central axis of the jet.

ent velocities obtained by independent observations (Abraham et al 1996). We can derive the viewing angle of the jet from the Doppler effect by equation as $\theta_{max} = 2arctan\frac{1}{\beta_{app}}$, where θ_{max} is the upper limit of the viewing angle between jet and line of sight. The θ_{max} for components C1, C2 and C3 is 19°.2 ± 0°.1, 21°.5 ± 0°.1, and 15°.7 ± 0°.1, respectively.

3.2. RM distribution

The longer integration time towards 3C 273 at this epoch compare to the first epoch bring us good *uv* coverage, then we could reveal the distribution of the RM on a large part of the jet. We also detected a gradient of RM across the jet in this epoch. The value of RM are typical a few hundred rad m^{-2}, and the value of RM at the left hand side is larger than that at right hand side. It is consistent with our previous results (KA02) and independent results by Zavala & Taylor (2004). The gradients of RM across the jets continue for 20 mas in angular distance, which corresponds to 38.4 pc in the projected distance. Taking account for the viewing angle of the jet of component C2 of 21.°5, The linear distance is longer than 100 pc.

We show the cross-section of RM along several lines perpendicular to the jet in figure 2.

4. Discussion

4.1. Time evolution of RM

In order to investigate the time evolution of the RM distribution, we tentatively shifting the distribution of RM of the first epoch by pixel to pixel in both R.A. and Dec, and calculated "reduced-χ^2" at each shifted position. We used the pixels where both distributions of RM have a significant value (SNR > 3), and limited the calculation whereas amount of the integrated area is larger than three times of the synthesized beam size of the first epoch. The values of RM at each pixel are not independent of that at the next pixel due to convolution of the synthesized beam. We cannot calculate exact value of reduced-χ^2, since we cannot know the degree of freedom. We think, however, that the relative value in the distribution is still useful in order to discuss the relative position. It gives the distribution being similar to each other. The resultant χ^2 distribution is shown in figure 3.

The distribution of the "reduced-χ^2" shows smooth features and is minimum at when the distribution of RM at the first epoch is shifted 5.5 mas in R.A. and − 2.5 mas in Dec relative to that of the second epoch. Since we could reveal the distribution of RM on only component C2 in the first epoch, we think that this analysis evaporates the time evolution of RM at component C2. The amount of the shift probably indicates the time variation of the magnetized plasma that causes of the RM of component C2 and is 5.5 mas to the west and 2.5 mas to the south, corresponding to the proper motion being 5.25 c at the position angle of 245°.6. This is coincidentally well consistent

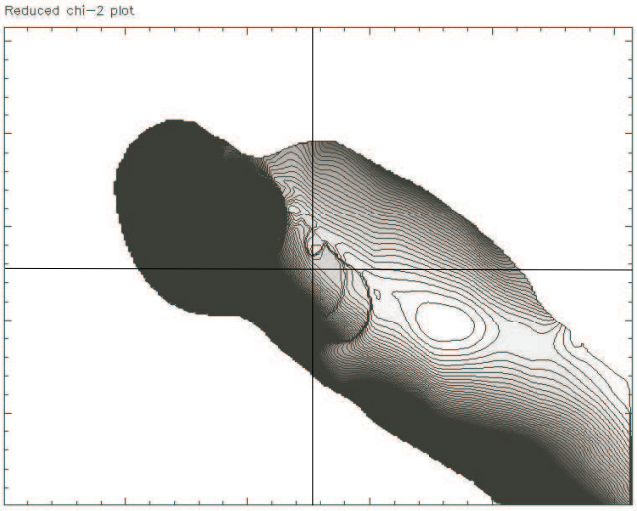

Fig. 3. Distribution of the modified "reduced-χ^2". The cross point of the vertical and horizontal line indicate the registration at the normal position. Both contour and grey scale indicate "reduced-χ^2". For the grey scale, black color indicate high "reduced-χ^2" and white color indicate low "reduced-χ^2". The minimum "reduced-χ^2" is obtained when the distribution of RM at the first epoch is shifted 5.5 mas to the R.A. direction and − 2.5 mas to the Dec direction relative to that of the second epoch. It corresponds to the proper motion of 5.25 c, which is coincidentally almost consistent with the apparent proper motion of component C2 of 5.26 ± 0.01 c.

with the apparent proper motion of component C2 of 5.26 ± 0.01 c at the position angle of 239°.6, which strongly suggests that the magnetized plasma is associated with component C2.

4.2. Origin of RM

The variation of the RM can not be associated with foreground Faraday screen, since we consider about mill-arcsecond scale fluctuation of RM. In addition, we detected time variation of RM towards jet. Evaporation of the time variance would be important to discriminate origin of the RM. We considered two cases for the origin of the RM; magnetized plasma in the Narrow Line Region (NLR), and magnetized plasma associated with the jet itself.

It is well-known that magnetized plasma in the NLR typically have the velocity of 1000 km s^{-1}. At the distance of 3C 273, this motion corresponds to 0.00056 mas yr^{-1}. The estimated motion between the two epochs (7 years) is 0.004 mas. It is too small compared to the beam size, and this does not affect the time variation of the RM. Also, the internal change of the magnetized plasma can be origin of the time variation of the RM and it should be due to the change of the density of the magnetized plasma and/or magnetic field. Then the characteristic time scale of the change of RM should be related with the size of magnetized plasma and sound velocity or Alfvén velocity. Assuming a plasma temperature in NLR of 10^4 K and an equipartition condition for the magnetic pressure and thermal pressure, we estimate the Alfvén velocity and the sound speed as 0.00004 c and 0.00007 c, respectively. If we assume a scale length of the magnetized plasma of 1 pc, a typical time scale of the variation of RM due to the change of density and line of sight component of the magnetic field is estimated at 8×10^4 years and 4×10^4 years, respectively. Therefore we think these possibilities are unlikely for the origin of the RM.

On the other hand, the amount of the shift is coincidentally corresponds to the motion of the emitting plasma. Thus it is natural to think that magnetized plasma that make the RM gradient can be a part of the jet, and gradient of the RM would be related with the helical magnetic field as discussed in KA02. RM occur in the magnetized plasma consists of low γ electrons and protons (Kennett & Melrose 1998). It would be difficult to accelerate cold plasma consist of electrons and protons up to a balk Lorentz factor of at least 5.25.

5. Conclusions

In order to obtain more evidences for the helical magnetic field in the 3C 273 jet, we made a follow-up VLBA polarimetry. We could revealed the distribution of the RM on the most of the part of the VLBI jet, and there are transverse gradient of RM same as the results of previous observation, but we could revealed longer jet of 38.4 pc in the projected distance. In addition, the pattern of the distribution of RM shows time variation, and its motion coincidentally corresponds to that of the emitting plasma of 5.26 c. These results indicates the presence of the helical magnetic field more strongly.

Acknowledgements. This research has made use of data taken by Very Long Baseline Array (VLBA). VLBA is operated by the National Radio Astronomy Observatory (NRAO), and NRAO is a facility of the National Science Foundation operated under cooperative agreement by Associated Universities, Inc.

References

Abraham, Z., Carrara, E.A., Zensus, J.A., & Unwin, S.C. 1996, A&AS, 115, 543
Asada, K., et al. 2002, PASJ, 54, 39L
Blandford, R. D. & Konigl, A. 1979, ApJ, 232, 34
Cohen, M. H., Cannon, W., Purcell, G. H., Shaffer, D. B., Broderick, J. J., Kellermann, K. I. & Jauncey, D. L. 1971, ApJ, 170, 207
Gabuzda, D. C. 2000, Astrophysical Phenomena Revealed by Space VLBI, Proceedings of the VSOP Symposium, held at the Institute of Space and astronautical Science, Sagamihara, Kanagawa, Japan, January 19 - 21, 2000, Eds.: H. Hirabayashi, P.G. Edwards, and D.W. Murphy, Published by the Institute of Space and Astronautical Science, p. 121
Gabuzda, D. C., Pushkarev, A. B., & Cawthorne, T. V. 2000, MNRAS, 319, 1109
Gabuzda, D. C., Murray, E. & Cronin, P. 2004, MNRAS, 351, L89
Junor, W., Biretta, J. A. & Livio, M. 1999, Natur, 401, 891
Kennett, M. P. & Melrose, D. B. 1998 PhRvD, 58, 3011
Meier, D. L., Koide, S. & Uchida, Y. 2001, Sci, 291, 84
Schmidt, M. 1963, Nature, 197, 1040
Sikora, M., Sol, H., Begelman, M. C. & Madejski, G. M. 1996MNRAS, 280, 781S 1996, A&AS, 120, 579
Whiteny, A. R., Shapiro, I. I., Rogers, A. E. E., Robertson, D. S., Knight, C. A., Clark, T. A., Goldstein, R. M., Marandino, G. E. et al. 1971, Science, 173. 225
Zavala, R.T. & Taylor, G.B. 2004, astro-ph/0405534